

Characterization of a thermostable 2,4-diaminopentanoate dehydrogenase from *Fervidobacterium nodosum* Rt17-B1

Sadanobu Fukuyama,<sup>1</sup> Hisaaki Mihara,<sup>1</sup> Ryoma Miyake,<sup>2,3</sup> Makoto Ueda,<sup>2,3</sup> Nobuyoshi Esaki,<sup>1</sup> and Tatsuo Kurihara<sup>1,\*</sup>

<sup>1</sup>Institute for Chemical Research, Kyoto University, Uji, Kyoto 611-0011, Japan

<sup>2</sup>Mitsubishi Chemical Group Science and Technology Research Center, Inc., Yokohama 227-8502, Japan

<sup>3</sup>API Corporation, Yokohama 227-8502, Japan

\*Corresponding author. Tel: +81-774-38-4710, Fax: +81-774-38-3248, E-mail: kurihara@scl.kyoto-u.ac.jp

Present addresses.

S. F.: KOGA ISOTOPE, Ltd., Koka, Shiga 520-3404, Japan

H. M.: Department of Biotechnology, College of Life Sciences, Ritsumeikan University, Kusatsu, Shiga 525-8577, Japan

M. U.: Department of Materials Chemistry and Bioengineering, Oyama National College of Technology, Oyama, Tochigi 323-0806, Japan

Running title: Thermophilic 2,4-diaminopentanoate dehydrogenase

Key words: 2,4-diaminopentanoate dehydrogenase; *Fervidobacterium nodosum*; amino acid dehydrogenase; ornithine metabolism; deamination; amination; thermophilic enzyme

## Abstract

2,4-Diaminopentanoate dehydrogenase (2,4-DAPDH), which is involved in the oxidative ornithine degradation pathway, catalyzes the  $\text{NAD}^+$ - or  $\text{NADP}^+$ -dependent oxidative deamination of (2*R*, 4*S*)-2,4-diaminopentanoate (2,4-DAP) to form 2-amino-4-oxopentanoate. A *Fervidobacterium nodosum* Rt17-B1 gene, *Fnod\_1646*, which codes for a protein with sequence similarity to 2,4-DAPDH discovered in metagenomic DNA, was cloned and overexpressed in *Escherichia coli*, and the gene product was purified and characterized. The purified protein catalyzed the reduction of  $\text{NAD}^+$  and  $\text{NADP}^+$  in the presence of 2,4-DAP, indicating that the protein is a 2,4-DAPDH. The optimal pH and temperature were 9.5 and 85°C, respectively, and the half-denaturation time at 90°C was 38 min. Therefore, the 2,4-DAPDH from *F. nodosum* Rt17-B1 is an  $\text{NAD(P)}^+$ -dependent thermophilic-alkaline amino acid dehydrogenase. This is the first thermophilic 2,4-DAPDH reported, and it is expected to be useful for structural and functional analyses of 2,4-DAPDH and for the enzymatic production of chiral amine compounds. Activity of 2,4-DAPDH from *F. nodosum* Rt17-B1 was suppressed by 2,4-DAP via uncompetitive substrate inhibition. In contrast, the enzyme showed typical Michaelis-Menten kinetics toward 2,5-diaminohexanoate. The enzyme was uncompetitively inhibited by D-ornithine with an apparent  $K_i$  value of 0.1 mM. These results suggest a regulatory role for this enzyme in the oxidative ornithine degradation pathway.

## Introduction

2,4-Diaminopentanoate dehydrogenase (2,4-DAPDH, EC 1.4.1.12) catalyzes  $\text{NAD}^+$ - or  $\text{NADP}^+$ -dependent oxidative deamination of (2*R*, 4*S*)-2,4-diaminopentanoate (2,4-DAP) at carbon 4 to form 2-amino-4-oxopentanoate (AKP) (1). In the 1970s, this enzyme was first discovered in a crude extract of *Clostridium sticklandii* as a part of the oxidative ornithine degradation pathway (Fig. 1) (2-4), and the genes implicated in this pathway were recently identified through a metagenomics approach in an anaerobic digester from a wastewater treatment plant (5). The oxidative ornithine degradation pathway has also been verified in several anaerobic genera, including *Clostridium*, *Thermoanaerobacter*, *Propionibacterium*, and *Fervidobacterium*. The first step in this pathway is the conversion of L-ornithine to the D isomer by ornithine racemase (6). D-Ornithine is then converted to 2,4-DAP by D-ornithine aminomutase (OAM), an adenosylcobalamine (AdoCbl) and pyridoxal phosphate (PLP)-dependent enzyme, in which the amino group at carbon 5 is migrated to carbon 4 (7). 2,4-DAP is then oxidatively deaminated to form AKP. In the final step in this pathway, AKP undergoes a thiolytic cleavage, which is catalyzed by AKP thiolase with coenzyme A, to form acetyl-CoA and D-alanine (8).

Chiral amines are important starting materials for the synthesis of pharmaceuticals and agrochemicals. To obtain these chiral amine compounds, a variety of chemical and enzymatic methods have been utilized. Some examples include the enzymatic synthesis of chiral amines with lipases (9, 10) and  $\omega$ -amino acid aminotransferases (11, 12). One drawback of most of these strategies is that they require auxiliary compounds and involve multistep transformations. In addition, in synthesis methods using an aminotransferase, the yield of the product is often unsatisfactory due to the reaction equilibrium. These drawbacks may be overcome by using amino acid dehydrogenases. Amino acid dehydrogenases catalyze the reduction of  $\alpha$ -keto acids with concomitant amination of the substrates with  $\text{NAD(P)H}$  and an ammonium ion. Therefore, these enzymes are useful for producing chiral amines from the corresponding  $\alpha$ -keto acid compounds in one step along with an established

NAD(P)H recycling system. The product yield might also be enhanced by increasing the concentration of NAD(P)H with an NAD(P)H regeneration system. However, despite these advantages, the applications for amino acid dehydrogenases have been limited to the production of  $\alpha$ -amino acids. 2,4-DAPDH may expand the application range of amino acid dehydrogenases for the production of other chiral amine compounds, because 2,4-DAPDH should catalyze the amination of the carbonyl group at the  $\gamma$  position.

Thermostable enzymes from thermophilic organisms have been used extensively in industry because these enzymes are inherently stable in harsh industrial processes. *Fervidobacterium* belongs to the eubacterial order of *Thermotogales*, which includes the most extremely thermophilic eubacteria presently known. It can grow at temperatures above 60°C with an optimal temperature of approximately 80°C (13). In this study, we carried out gene cloning, overexpression, purification, and biochemical characterization of a thermostable 2,4-DAPDH from the thermophilic anaerobic bacterium, *Fervidobacterium nodosum* Rt17-B1. This is the first report of a thermophilic 2,4-DAPDH. The role of this enzyme in the oxidative ornithine degradation pathway is also discussed.

## 87 Materials and Methods

### 88 *Materials*

89 Restriction enzymes and kits for genetic manipulation were obtained from Takara Bio  
90 (Kyoto, Japan), New England Biolabs (Ipswich, MA), and Stratagene (La Jolla, CA). The pET14b  
91 expression vector was purchased from Novagen (Madison, WI). His-bind Resin was obtained from  
92 Novagen. All other reagents were of analytical grade and were from Nacalai Tesque (Kyoto, Japan)  
93 and Wako Pure Chemical Industries (Osaka, Japan).

94

### 95 *Cloning of the 2,4-DAPDH gene from F. nodosum Rt17-B1*

96 Genomic DNA was isolated from *F. nodosum* Rt17-B1 (DSMZ, Braunschweig, Germany)  
97 using a DNeasy Blood & Tissue Kit (Qiagen, Venlo, Netherlands) according to the manufacturer's  
98 instructions. The gene encoding 2,4-DAPDH was amplified by overlap extension PCR to remove the  
99 intrinsic NdeI site in the coding region. Two separate amplification reactions were performed using  
100 Phusion DNA polymerase (Finnzymes, Espoo, Finland), 100 ng of genomic DNA as a template, and  
101 the following two sets of primers: Fnod\_1646 NdeI N  
102 (5'-GCGGGAATTCCCATATGCGTATAGTTACTTGGGG-3') and Fnod\_1646 deNdeI R  
103 (5'-CATTTATCGCCAACCGTATGCTTTTGCTG-3') to amplify the DNA coding for the N-terminal  
104 part of the protein, and Fnod\_1646 deNdeI F (5'-CAGCAAAAGCCATACGTTGGCGATAAATG-3')  
105 and Fnod\_1646 BamHI C (5'-GCCGCGGATCCTCATTCCATTGAGAAAGGATTG-3') to amplify  
106 the DNA coding for the C-terminal part of the protein. The underlined sequences indicate the  
107 restriction sites for NdeI and BamHI, respectively. The double-underlined sequences indicate the sites  
108 that anneal to the intrinsic NdeI site in the coding region. The PCR products were mixed and used as  
109 templates in a second PCR to amplify the full-length gene using Fnod\_1646 NdeI N and Fnod\_1646  
110 BamHI C. The amplified product was digested with NdeI and BamHI and inserted into the  
111 corresponding sites of pET14b to generate an N-terminal His6-tagged protein. The recombinant

112 plasmid was designated pET\_Fnod\_DAPDH.

113

#### 114 *Expression and purification of 2,4-DAPDH*

115 pET\_Fnod\_DAPDH was introduced into *Escherichia coli* Rosetta (DE3), and the cells were  
116 grown in LB medium containing 0.1 mM IPTG at 28°C for 15–17 h. The cells were harvested by  
117 centrifugation, resuspended in 50 mM Tris-HCl (pH 8.0), and homogenized by sonication. The  
118 homogenate was centrifuged at  $25,000 \times g$  for 40 min at 4°C. The supernatant was loaded onto a  
119 His-bind column (10 mL) equilibrated with 50 mM Tris-HCl (pH 8.0). The enzyme was eluted with a  
120 600-mL linear gradient of 0–500 mM imidazole in the same buffer. The enzyme fractions were pooled  
121 and dialyzed against 50 mM Tris-HCl (pH 8.0). The final preparation of the enzyme was stored at  
122 -80°C until use.

123

#### 124 *Synthesis of 2,4-DAP*

125 2,4-DAP was obtained from D-ornithine by enzymatic synthesis using OAM. To prepare  
126 OAM, which is comprised of two subunits, OraS and OraE, the genes coding for these subunits were  
127 amplified by PCR from *F. nodosum* genomic DNA using the following two sets of primers:  
128 FnodOAMS\_N\_Bam (5'-GGAGGGGATCCGATGAAACCAAGGCCG-3') and  
129 FnodOAMS\_C\_Hind (5'-TTTTCTTGGGTCGAGTTAAGCTTTTATTTAC-3') for *oraS* and  
130 FnodOAME\_N\_Nde (5'-GCGGTGAGTAACATATGGACAAAC-3') and FnodOAME\_C\_Xho  
131 (5'-GAATTTGACTCGAGTTATTTTTGAGATTC-3') for *oraE*. The underlined sequences indicate  
132 the restriction sites for BamHI, HindIII, NdeI, and XhoI, respectively. The *oraS* PCR product was  
133 digested with BamHI and HindIII and inserted into the corresponding sites of Multiple cloning site-1  
134 of pCOLA Duet-1, and the *oraE* PCR product was digested with NdeI and XhoI and inserted into the  
135 corresponding sites of Multiple cloning site-2 of the same plasmid. The recombinant plasmid was  
136 designated pCOLA\_Fnod\_OAM.

137 *E. coli* Rosetta (DE3) cells harboring the expression plasmid pCOLA\_Fnod\_OAM were  
138 grown in LB medium containing 0.1 mM IPTG at 28°C for 15–17 h. The cells were harvested by  
139 centrifugation, resuspended in a 25-mM ACES buffer (pH 6.5), and homogenized by sonication. The  
140 homogenate containing OAM was used to synthesize 2,4-DAP from D-ornithine.

141 The reaction mixture for the synthesis of 2,4-DAP consisted of 25 mM ACES buffer (pH  
142 6.5), 50 mM D-ornithine, 50 μM PLP, 50 μM AdoCbl, 1 mM DTT, and the homogenate. The reaction  
143 was performed in the dark on a magnetic stirrer plate at 55°C for 21 h. The reaction was terminated by  
144 the addition of trichloroacetic acid (final concentration, 25%). After centrifugation and three ether  
145 extractions, the extract was evaporated and taken up in water. The solution was desalted with a  
146 Dowex-50W-X8, 200 to 400 mesh, H<sup>+</sup>-form column. After washing, the D-ornithine and 2,4-DAP  
147 adsorbed to the column were eluted with 1 M NH<sub>4</sub>OH. The D-ornithine and 2,4-DAP fractions were  
148 pooled, evaporated, and reconstituted in chloroform:methanol:15% NH<sub>4</sub>OH (36:46:20). D-Ornithine  
149 and 2,4-DAP were then separated by column chromatography by using silicic acid (Silica Gel 60, 100  
150 to 210 mesh; KANTO CHEMICAL, Tokyo, Japan) with chloroform:methanol:15% NH<sub>4</sub>OH (36: 46:  
151 20). The 2,4-DAP fractions were pooled and evaporated.

152

#### 153 *Synthesis of 2,5-diaminohexanoate (2,5-DAH)*

154 2,5-DAH was obtained from D-lysine by enzymatic synthesis with lysine 5,6-aminomutase.  
155 To obtain the enzyme, which is comprised of two subunits, KamD and KamE, the genes coding for  
156 these subunits were amplified from *Thermoanaerobacter tengcongensis* genomic DNA by PCR using  
157 the following two sets of primers: TTELAMa\_N\_Bam  
158 (5'-GAGGGGATCCGATGAAGAAGAGCAAG-3') and TTELAMa\_C\_Sal  
159 (5'-GGCGTCGACTCATCCTCTATCACCTCTT-3') for *kamD* and TTELAMb\_N\_Nde  
160 (5'-GGTGATAGCATATGAACAGCGG-3') and TTELAMb\_C\_Xho  
161 (5'-AATCGGCTCGAGTTATTTTTTATACCCTT-3') for *kamE*. The underlined sequences indicate

the restriction sites for BamHI, SalI, NdeI, and XhoI, respectively. The *kamD* PCR product was digested with BamHI and SalI and inserted into the corresponding sites in Multiple cloning site-1 of pCOLA Duet-1. The *kamE* PCR product was digested with NdeI and XhoI and inserted into the corresponding sites in Multiple cloning site-2 of the same plasmid. The recombinant plasmid was designated pCOLA\_TTE\_LAM.

*E. coli* Rosetta (DE3) cells harboring the expression plasmid pCOLA\_TTE\_LAM were grown in LB medium containing 0.1 mM IPTG at 28°C for 15–17 h. The cells were harvested by centrifugation, suspended in 25 mM PIPES buffer (pH 6.5), and homogenized by sonication. The homogenate containing lysine 5,6-aminomutase was used to synthesize 2,5-DAH from D-lysine.

The reaction mixture for the synthesis of 2,5-DAH consisted of 25 mM PIPES buffer (pH6.5), 50 mM D-lysine, 50  $\mu$ M PLP, 50  $\mu$ M AdoCbl, 1 mM DTT, and the homogenate. The reaction was performed in the dark on a magnetic stirrer plate at 55°C for 21 h. The reaction was terminated by the addition of trichloroacetic acid (final concentration, 25%). After centrifugation and three ether extractions, the supernatant was concentrated by evaporation and taken up in water. The solution was desalted by using a Dowex-50W-X8, 200 to 400 mesh, H<sup>+</sup>-form column. After washing, the D-lysine and 2,5-DAH adsorbed to the column were eluted with 1 M NH<sub>4</sub>OH. The D-lysine and 2,5-DAH fractions were pooled, evaporated, and reconstituted in chloroform:methanol:15% NH<sub>4</sub>OH (6:70:20). D-Lysine and 2,5-DAH were then separated by column chromatography using silicic acid (Silica Gel 60, 100 to 210 mesh; KANTO CHEMICAL) with chloroform:methanol:15% NH<sub>4</sub>OH (6:70:20). The 2,5-DAH fractions were pooled and evaporated.

#### *Enzyme assay*

The activity of 2,4-DAPDH was determined spectrophotometrically by monitoring the change in A<sub>340</sub> upon the reduction of NAD<sup>+</sup> at 55°C. The assay mixture consisted of 0.5 mM NAD<sup>+</sup>, 0.5 mM substrate, and 50 mM HEPES-NaOH (pH 8.5). The reaction was started by the addition of the



187 enzyme.

188

#### 189 *Determination of optimal pH and temperature*

190 The pH optimum of the enzyme was determined using the following four buffer systems: 50  
191 mM acetate buffer (pH 5–5.5), 50 mM potassium phosphate buffer (KPB) (pH 5.5–7), HEPES-NaOH  
192 buffer (pH 7–8.5), and CHES-NaOH buffer (pH 8.5–10). The optimal temperature of the enzyme was  
193 determined by measuring the enzyme activity over the temperature range of 5°C–95°C.

194

#### 195 *Determination of thermostability*

196 The stability of the 2,4-DAPDH enzyme at elevated temperatures was investigated by  
197 incubating the enzyme in 50 mM HEPES-NaOH (pH 8.5) at 90°C and 100°C. At certain time intervals,  
198 samples were withdrawn, and the residual activity was measured under standard assay conditions.

199

#### 200 *Effect of metal ions and reagents*

201 The effects of metal ions and various reagents on the enzyme were determined by measuring  
202 activity after incubating it in 50 mM HEPES-NaOH (pH 8.5) with and without different metal ions and  
203 reagents at 0.5 mM.

204

#### 205 *Determination of kinetic parameters*

206 The initial rates of the enzyme reaction were measured while varying the concentration of  
207 one substrate while the concentration of the other substrate was held constant (and in excess). Data  
208 were fitted to the Michaelis-Menten equation, and the kinetic parameters were calculated using  
209 nonlinear least-squares regression with Kaleida Graph software (Adelbeck Software, Reading, PA).  
210 Substrate inhibition studies were performed with various concentrations of 2,4-DAP and a fixed  
211 saturating concentration of NAD<sup>+</sup> (0.5 mM). The data were fitted to Equation 1, which is the standard

212 equation for complete uncompetitive substrate inhibition.

213 
$$v = V_{\max} / \{1 + (K/[S]) + ([S]/K_i)\} \quad (\text{Equation 1})$$

214 In Equation 1,  $v$  and  $V_{\max}$  are the initial and maximum velocities, respectively,  $[S]$  is the substrate  
215 concentration,  $K$  is Michaelis constant for the substrate, and  $K_i$  is the inhibition constant for the  
216 substrate.

217 Inhibitor studies of 2,4-DAPDH employed the assay described above. The kinetic analysis  
218 was conducted with various concentrations of 2,4-DAP (0.01, 0.025, 0.05, 0.1, and 0.2 mM) and  
219 D-ornithine (0.5, 1.5, and 2.0 mM). The  $K_i$  value was calculated from the Dixon plot.

220

221

## 222 Results

### 223 *Identification and characterization of 2,4-DAPDH from F. nodosum Rt17-B1*

224 To obtain a 2,4-DAPDH with superior thermostability, we focused on the thermophilic  
225 bacterium *F. nodosum* Rt17-B1. This strain was believed to have a functional oxidative degradation  
226 pathway for ornithine because it has *oraS* and *oraE* homologues that encode the S and E subunits of  
227 ornithine aminomutase, respectively. In the genome sequence of *F. nodosum*, the candidate gene for  
228 2,4-DAPDH, *Fnod\_1646* (GenBank accession number: ABS61481.1), is adjacent to the *oraS* and  
229 *oraE* homologues. The putative protein encoded by *Fnod\_1646* is a homologue of the 2,4-DAPDH  
230 found in a metagenome from an anaerobic digester at a waste water-treatment plant (58.0% identity),  
231 which has been described as a homodimer with a subunit molecular mass of approximately 36 kDa that  
232 catalyzes the NAD<sup>+</sup>-dependent oxidation of 2,4-DAP to AKP. The protein encoded by *Fnod\_1646* has  
233 a predicted molecular mass of 38 kDa and the GXGXXG sequence motif characteristic of the  
234 Rossmann fold, which is a typical of NAD(P)<sup>+</sup>-binding proteins.

235 To examine the enzyme activity of this protein, the *Fnod\_1646* gene was cloned into the  
236 pET14b expression plasmid to construct pET\_Fnod\_DAPDH, and then heterologously expressed  
237 under the control of the T7 promoter in *E. coli* Rosetta (DE3) as an N-terminal His-tagged fusion. The  
238 gene product was purified in a single step by Ni-affinity chromatography. The homogeneity of the  
239 purified protein was verified by SDS-PAGE, which showed a single band with an apparent molecular  
240 mass of 38 kDa. In a reaction mixture containing 2,4-DAP, the purified protein catalyzed the reduction  
241 of NAD<sup>+</sup> to NADH, indicating that the protein is a 2,4-DAPDH.

242

### 243 *Optimal pH and thermostability*

244 To determine the optimal pH for 2,4-DAPDH, the activity of the enzyme was measured at  
245 55°C using 2,4-DAP as a substrate at pH 5.0–10. It showed maximum activity at pH 9.5 and high  
246 activity (>70% of maximum activity) at alkaline pHs in the range of 9.0–10.0 (Fig. 2). Enzymatic

activity was routinely determined at pH 8.5 (HEPES-NaOH buffer) in this study because NAD<sup>+</sup> is unstable at pH 9.0–10.0.

To determine the effect of temperature on enzyme activity, reactions were conducted using 2,4-DAP as a substrate in 50 mM HEPES-NaOH buffer (pH 8.5) over a temperature range of 5°C–95°C. The enzyme showed maximum activity at 85°C (Fig. 3). To test the thermostability of 2,4-DAPDH, the enzyme was incubated at 90°C and 100°C, and the residual activity was assayed. The half-life of the enzyme was estimated to be 38 min at 90°C and 2 min at 100°C (data not shown).

#### *Effect of various reagents on 2,4-DAPDH activity*

2,4-DAPDH activity was measured in the presence of EDTA and various divalent metal ions at a concentration of 0.5 mM (Table 1). EDTA did not affect 2,4-DAPDH activity. Mn<sup>2+</sup> had no significant effect on 2,4-DAPDH activity, whereas Mg<sup>2+</sup>, Ca<sup>2+</sup>, Fe<sup>2+</sup>, and Co<sup>2+</sup> moderately inhibited the activity, and Ni<sup>2+</sup>, Cu<sup>2+</sup>, and Zn<sup>2+</sup> almost completely inhibited the activity. Adding EDTA to the reaction mixture at a concentration equal to that of the metal ion completely suppressed the inhibition, indicating that these metals reversibly inactivated the enzyme (data not shown). K<sup>+</sup> and anions of the salts shown in Table 1 did not affect enzyme activity.

#### *Coenzyme and substrate specificity*

The coenzyme specificity of 2,4-DAPDH was examined by measuring enzyme activity using 2,4-DAP as a substrate and either NAD<sup>+</sup> or NADP<sup>+</sup> as the coenzyme. The experiment showed that the enzyme uses both NAD<sup>+</sup> and NADP<sup>+</sup> as a coenzyme (92 and 17 μmol·min<sup>-1</sup>·mg<sup>-1</sup>, respectively). However, the activity of the enzyme with NAD<sup>+</sup> was 5.4 times higher than that with NADP<sup>+</sup>. Therefore, the enzyme prefers to use NAD<sup>+</sup> as a coenzyme.

The substrate specificity of the enzyme during NAD<sup>+</sup>-dependent oxidative deamination was examined using 0.5 mM 2,4-DAP or 2,5-DAH. 2,5-DAH is produced by lysine 5,6-aminomutase,

which catalyzes the 5,6-rearrangement of the terminal amino group of D-lysine in the lysine degradation pathway (Fig. 1). 2,4-DAPDH from *F. nodosum* acted not only on 2,4-DAP (92  $\mu\text{mol}\cdot\text{min}^{-1}\cdot\text{mg}^{-1}$ ) but also on 2,5-DAH (1  $\mu\text{mol}\cdot\text{min}^{-1}\cdot\text{mg}^{-1}$ ). The activity of the enzyme using 2,4-DAP as a substrate was approximately 90 times higher than that using 2,5-DAH.

#### *Kinetic parameters of 2,4-DAPDH*

Kinetic analysis of the enzyme was performed using 0.005–1 mM  $\text{NAD}^+$  or 0.1–8 mM  $\text{NADP}^+$  as a coenzyme. The kinetic parameters determined are shown in Table 2. The  $K_m$  value for  $\text{NAD}^+$  was about 40 times lower than that for  $\text{NADP}^+$ , whereas the  $V_{\text{max}}$  and  $k_{\text{cat}}$  values for  $\text{NAD}^+$  and  $\text{NADP}^+$  were similar.

The activities of the enzyme were measured at various concentrations of 2,4-DAP and 2,5-DAH. The enzyme displayed non-Michaelis-Menten kinetics with 2,4-DAP as the substrate. Although the enzymatic activity increased as the 2,4-DAP concentration increased over the range of 0–0.8 mM, it decreased at 2,4-DAP concentrations over 0.8 mM (Fig. 4). This behavior is consistent with complete uncompetitive substrate inhibition, and the experimental data are fitted well by the equation describing this type of inhibition (Equation 1 in the Materials and Methods). An apparent  $K_i$  value and  $K_m$  value were calculated as 0.9 mM and 0.2 mM, respectively (Table 2). In contrast, the enzyme displayed typical Michaelis-Menten kinetics when 2,5-DAH (0–10 mM) was used as the substrate (Fig. 5). The kinetic parameters for these substrates are summarized in Table 2.

#### *Regulation of 2,4-DAPDH*

We examined whether the activity of 2,4-DAPDH is affected by D-ornithine and D-alanine, which occur as metabolites in the oxidative ornithine degradation pathway (Fig. 1). Enzyme activity was measured in a solution of 50 mM HEPES pH 8.5, 1 mM  $\text{NAD}^+$ , and 0.3 mM 2,4-DAP in the presence or absence of these amino acids. Enzymatic activity decreased to 14% and 71% of the

positive control in the presence of 5 mM D-ornithine and D-alanine, respectively. We also examined whether D-lysine affects enzyme activity under these same conditions. The activity decreased to 68% of the positive control following the addition of 5 mM D-lysine. Therefore, the activity of 2,4-DAPDH is suppressed in the presence of D-ornithine, D-alanine, and D-lysine. D-Ornithine is the most effective inhibitor. To further characterize the inhibition by D-ornithine, enzyme activity toward 2,4-DAPDH was measured in the presence of varying concentrations of D-ornithine. In double-reciprocal plots of enzyme activity versus 2,4-DAP concentration, a set of parallel linear lines were obtained (Fig. 6), indicating that D-ornithine acts as an uncompetitive inhibitor of 2,4-DAPDH. The apparent  $K_i$  value was 0.1 mM.

## 308 Discussion

309 In this paper, the gene cloning, expression, and characterization of a thermostable  
310 2,4-DAPDH from the thermophilic bacterium *F. nodosum* Rt17-B1 are described. The gene from this  
311 bacterium, *Fnod\_1646*, was predicted to encode a 2,4-DAPDH. The protein, which was purified from  
312 recombinant *E. coli* cells, showed a molecular mass of 38 kDa on SDS-PAGE and catalyzed the  
313 oxidative deamination of 2,4-DAP in an NAD(P)<sup>+</sup>-dependent manner. The optimum pH for 2,4-DAP  
314 oxidation was in the alkaline range. A variety of metals, such as Cu<sup>2+</sup>, Ni<sup>2+</sup>, and Zn<sup>2+</sup>, inhibited its  
315 catalytic activity. This 2,4-DAPDH is noteworthy because it has a high optimal temperature and is  
316 thermostable. The optimal temperature for this enzyme in 2,4-DAP oxidation was 85°C. Therefore, the  
317 enzyme is an NAD(P)<sup>+</sup>-dependent thermophilic alkaline amino acid dehydrogenase.

318 We found that besides 2,4-DAP, 2,5-DAH can also serve as the substrate for 2,4-DAPDH  
319 (Table 2). 2,5-DAH may be produced from D-lysine by lysine-5,6-aminomutase (14), raising the  
320 possibility that 2,4-DAPDH also participates in lysine degradation (Fig. 1). However, the  $k_{cat}/K_m$  value  
321 of 2,4-DAPDH for 2,5-DAH is much lower than that for 2,4-DAP, implying that 2,5-DAH is not a  
322 physiological substrate of 2,4-DAPDH. The validity of this interpretation should be verified in future  
323 *in vivo* studies.

324 In this study, we found notable regulatory properties of 2,4-DAPDH, including  
325 uncompetitive substrate inhibition by 2,4-DAP and uncompetitive inhibition by D-ornithine. These  
326 results suggest that the oxidative degradation of ornithine is regulated by upstream metabolites; at high  
327 concentrations of D-ornithine and 2,4-DAP, this degradation pathway is suppressed. It is known that  
328 substrate inhibition of enzymes, such as tyrosine hydroxylase, plays a role in stabilizing the reaction  
329 rate against large fluctuations in substrate concentration (15). Therefore, upstream regulation of the  
330 oxidative ornithine degradation pathway may result in a steady synthesis of downstream metabolites,  
331 such as the D-alanine that is required for the synthesis of peptidoglycan (16, 17), under conditions at  
332 which the concentrations of the upstream metabolites fluctuate.

The regulation of 2,4-DAPDH may also affect the metabolic fate of ornithine, which may be metabolized via four different pathways, as analysis of the *F. nodosum* genome and previous reports suggested the occurrence of four ornithine metabolic pathways in this bacterium. The first is the oxidative degradation pathway that was the focus of this study. The second is a spermidine and spermine biosynthesis pathway, which starts with the conversion of L-ornithine into putrescine by ornithine decarboxylase. Polyamines, such as spermidine and spermine, are polycationic compounds that are implicated in a wide variety of biological reactions, including the synthesis of nucleobases and proteins (20). The third is the urea cycle in which ornithine is metabolized by ornithine carbamoyltransferase (19). The fourth is the reductive degradation pathway in which ornithine is reduced to 5-aminovalerate through the formation of proline (5). This reductive pathway has been found in anaerobic bacteria such as *C. sticklandii* (18). Inhibition of 2,4-DAPDH by the upstream metabolites in the oxidative ornithine degradation pathway may direct the metabolic flux of L-ornithine to other pathways. This should be examined in future studies by *in vivo* experiments.

Amino acid dehydrogenases are useful for the synthesis of chiral amino acids from the corresponding keto acids. Because most amino acid dehydrogenases characterized thus far catalyze the interconversion between  $\alpha$ -amino acids and  $\alpha$ -keto acids, this method has only been used for the production of chiral  $\alpha$ -amino acids. Based on its activity toward 2,4-DAP and 2,5-DAH, 2,4-DAPDH should catalyze the reductive amination of the carbonyl group at the  $\gamma$ -position and the  $\delta$ -position, which differs from the activity of most previously characterized amino acid dehydrogenases. In a preliminary experiment, we tested the reductive amination of 2,4-DAPDH using the oxidative deamination product of 2,4-DAP. After 2,4-DAP was converted to AKP, the reaction was stopped by heat treatment, and AKP was used as the substrate for reductive amination reaction. 2,4-DAPDH catalyzed the AKP-dependent oxidation of NADH, implying that the enzyme catalyzed the reductive amination of AKP (data not shown). Therefore, 2,4-DAPDH is expected to expand the range of chiral amine compounds (other than  $\alpha$ -amino acids) produced by amino acid dehydrogenases. When



358 considering such applications, the thermostability of the enzyme is beneficial. Possible applications in  
359 the synthesis of chiral amine compounds for the thermostable 2,4-DAPDH identified in this study are  
360 currently under investigation.

#### 361 362 Acknowledgments

363 This work was supported in part by the Collaborative Research Program of Institute for Chemical  
364 Research, Kyoto University (grant # 2013-59).

367 References

368

- 369 1. **Somack, R. and Costilow, R. N.:** 2,4-Diaminopentanoic acid C<sub>4</sub> dehydrogenase.  
 370 Purification and properties of the protein, J. Biol. Chem., **248**, 385-388 (1973).
- 371 2. **Dyer, J. K. and Costilow, R. N.:** 2,4-Diaminovaleric acid: an intermediate in the anaerobic  
 372 oxidation of ornithine by *Clostridium sticklandii*, J. Bacteriol., **101**, 77-83 (1970).
- 373 3. **Tsuda, Y. and Friedmann, H. C.:** Ornithine metabolism by *Clostridium sticklandii*.  
 374 Oxidation of ornithine to 2-amino-4-ketopentanoic acid via 2,4-diaminopentanoic acid; participation  
 375 of B<sub>12</sub> coenzyme, pyridoxal phosphate, and pyridine nucleotide, J. Biol. Chem., **245**, 5914-5926  
 376 (1970).
- 377 4. **Barker, H. A.:** Amino acid degradation by anaerobic bacteria, Annu. Rev. Biochem., **50**,  
 378 23-40 (1981).
- 379 5. **Fonknechten, N., Perret, A., Perchat, N., Tricot, S., Lechaplais, C., Vallenet, D., Vergne,**  
 380 **C., Zaparucha, A., Le Paslier, D., Weissenbach, J., and Salanoubat, M.:** A conserved gene cluster  
 381 rules anaerobic oxidative degradation of L-ornithine, J. Bacteriol., **191**, 3162-3167 (2009).
- 382 6. **Chen, H. P., Lin, C. F., Lee, Y. J., Tsay, S. S., and Wu, S. H.:** Purification and properties of  
 383 ornithine racemase from *Clostridium sticklandii*, J. Bacteriol., **182**, 2052-2054 (2000).
- 384 7. **Somack, R. and Costilow, R. N.:** Purification and properties of a pyridoxal phosphate and  
 385 coenzyme B<sub>12</sub> dependent D- $\alpha$ -ornithine 5,4-aminomutase, Biochemistry, **12**, 2597-2604 (1973).
- 386 8. **Jeng, I. M., Somack, R., and Barker, H. A.:** Ornithine degradation in *Clostridium*  
 387 *sticklandii*; pyridoxal phosphate and coenzyme A dependent thiolytic cleavage of  
 388 2-amino-4-ketopentanoate to alanine and acetyl coenzyme A, Biochemistry, **13**, 2898-2903 (1974).
- 389 9. **Torres-Gavilán, A., Escalante, J., Regla, I., López-Munguía, A., and Castillo, E.:**  
 390 'Easy-on, easy-off' resolution of chiral 1-phenylethylamine catalyzed by *Candida antarctica* lipase B,  
 391 Tetrahedron: Asymmetry, **18**, 2621-2624 (2007).

- 392 10. **Pilissão, C., Carvalho, P. O., and Nascimento, M. G.:** Enantioselective acylation of  
393 (*RS*)-phenylethylamine catalysed by lipases, *Process Biochem.*, **44**, 1352-1357 (2009).
- 394 11. **Koszelewski, D., Tauber, K., Faber, K., and Kroutil, W.:**  $\omega$ -Transaminases for the  
395 synthesis of non-racemic  $\alpha$ -chiral primary amines, *Trends Biotechnol.*, **28**, 324-332 (2010).
- 396 12. **Tufvesson, P., Lima-Ramos, J., Jensen, J. S., Al-Haque, N., Neto, W., and Woodley, J. M.:**  
397 Process considerations for the asymmetric synthesis of chiral amines using transaminases,  
398 *Biotechnol. Bioeng.*, **108**, 1479-1493 (2011).
- 399 13. **Patel, B. K. C., Morgan, H. W., and Daniel, R. M.:** *Fervidobacterium nodosum* gen. nov.  
400 and spec. nov., a new chemoorganotrophic, caldoactive, anaerobic bacterium, *Arch. Microbiol.*, **141**,  
401 63-69 (1985).
- 402 14. **Stadtman, T. C.:** Lysine metabolism by Clostridia, *Advance in Enzymology and Related*  
403 *Areas of Molecular Biology*, **38**, 413-448 (1973).
- 404 15. **Reed, M. C., Lieb, A., and Nijhout, H. F.:** The biological significance of substrate  
405 inhibition: a mechanism with diverse functions, *Bioessays*, **32**, 422-429 (2010).
- 406 16. **van Heijenoort, J.:** Formation of the glycan chains in the synthesis of bacterial  
407 peptidoglycan, *Glycobiology*, **11**, 25R-36R (2001).
- 408 17. **van Heijenoort, J.:** Recent advances in the formation of the bacterial peptidoglycan  
409 monomer unit, *Nat. Prod. Rep.*, **18**, 503-519 (2001).
- 410 18. **Kenklies, J., Ziehn, R., Fritsche, K., Pich, A., and Andreessen, J. R.:** Proline biosynthesis  
411 from L-ornithine in *Clostridium sticklandii*: purification of  $\Delta^1$ -pyrroline-5-carboxylate reductase, and  
412 sequence and expression of the encoding gene, *proC*, *Microbiology*, **145**, 819-826 (1999).
- 413 19. **Legrain, C., Stalon, V., Noullez, J. P., Mercenier, A., Simon, J. P., Broman, K., and**  
414 **Wiame, J. M.:** Structure and function of ornithine carbamoyltransferases, *Eur. J. Biochem.*, **80**,  
415 401-409 (1977).
- 416 20. **Tabor, C. W. and Tabor, H.:** Polyamines in microorganisms, *Microbiol. Rev.*, **49**, 81-99

417 (1985).

418

419

420 Figure Legends

421 Figure 1. The ornithine oxidative degradation pathway and putative lysine degradation pathway.  
422 Ornithine racemase, D-ornithine 4,5-aminomutase, 2,4-diaminopentanoate dehydrogenase,  
423 2-amino-4-ketopentanoate thiolase, lysine racemase, and D-lysine 5,6-aminomutase catalyze reactions  
424 1, 2, 3, 4, 5, and 6 respectively. Reaction 7 is non-enzymatic intramolecular cyclization.

425

426 Figure 2. Effect of pH on the activity of the 2,4-DAPDH from the thermophilic anaerobic bacterium, *F.*  
427 *nodosum* Rt17-B1. Enzyme assays were performed using 0.5 mM 2,4-DAP as the substrate in 50 mM  
428 acetate (filled circles), 50 mM KPB (open squares), HEPES-NaOH (filled triangles), and  
429 CHES-NaOH (filled diamonds) as described in the Materials and Methods. Error bars represent the  
430 standard deviation of three independent experiments.

431

432 Figure 3. Effect of temperature on the activity of 2,4-DAPDH. Enzyme assays were performed using  
433 0.5 mM 2,4-DAP as the substrate in 50 mM HEPES-NaOH (pH 8.5) at different temperatures as  
434 described in the Materials and Methods. Error bars represent the standard deviation of three  
435 independent experiments.

436

437 Figure 4. Substrate inhibition of 2,4-DAPDH by 2,4-DAP. 2,4-DAPDH activity is plotted as a function  
438 of 2,4-DAP concentration. The solid line is a fit to the data (filled circles) according to Equation 1 in  
439 the Materials and Methods.

440

441 Figure 5. Activity of 2,4-DAPDH toward 2,5-DAH. 2,4-DAPDH activity was plotted as a function of  
442 2,5-DAH concentration. The solid line is a fit to the data (filled diamonds) according to the  
443 Michaelis-Menten equation.

444

445 Figure 6. Inhibition of 2,4-DAPDH by D-ornithine. Double-reciprocal plots were generated at the  
446 following D-ornithine concentrations: 0 mM (filled diamonds), 0.5 mM (open circles), 1.5 mM (filled  
447 triangles), and 2.0 mM (open squares).

448

5. Figure 1

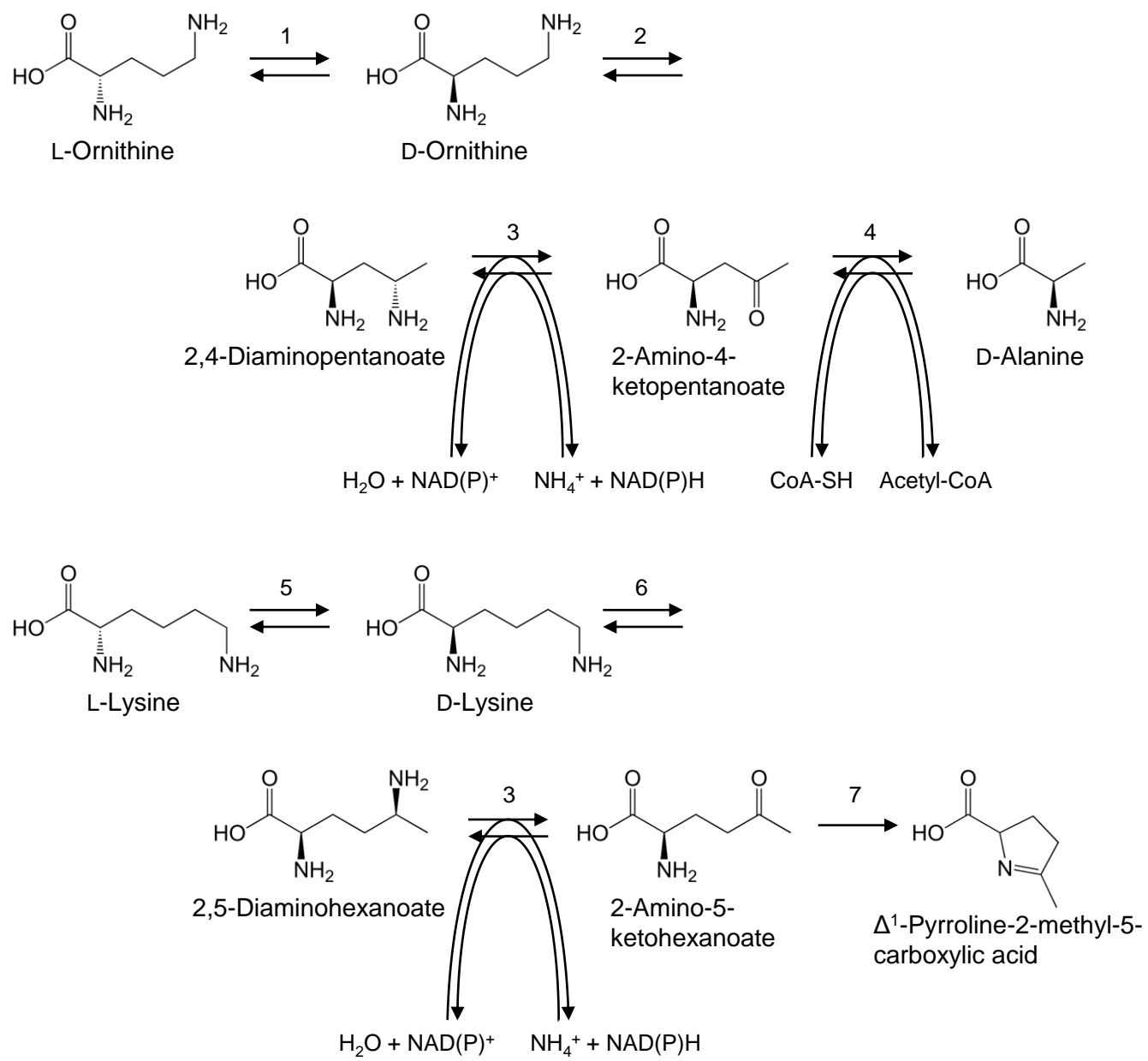


Figure 1

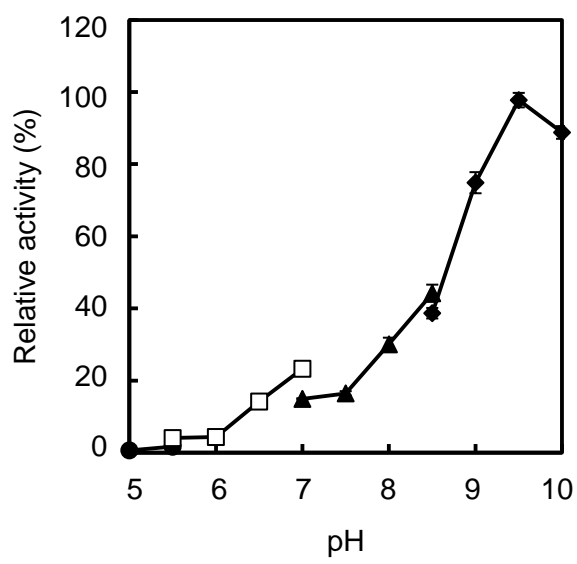


Figure 2



5. Figure 3

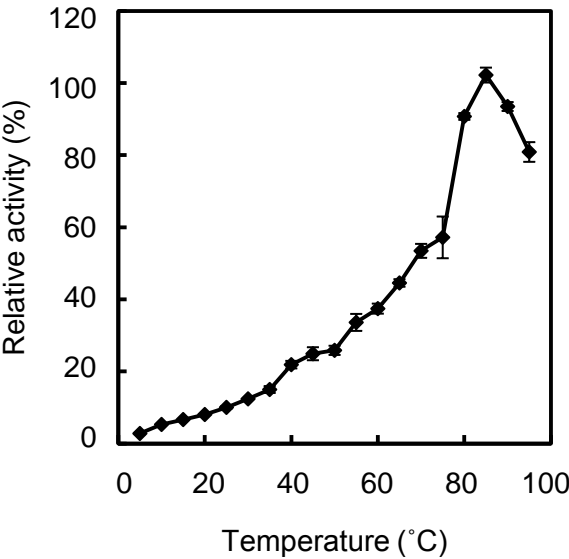


Figure 3

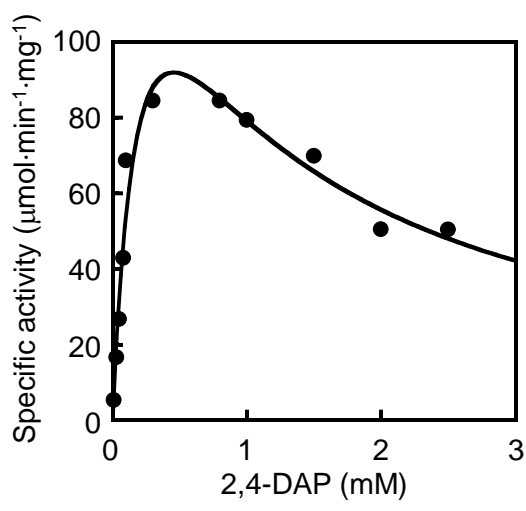


Figure 4

5. Figure 5

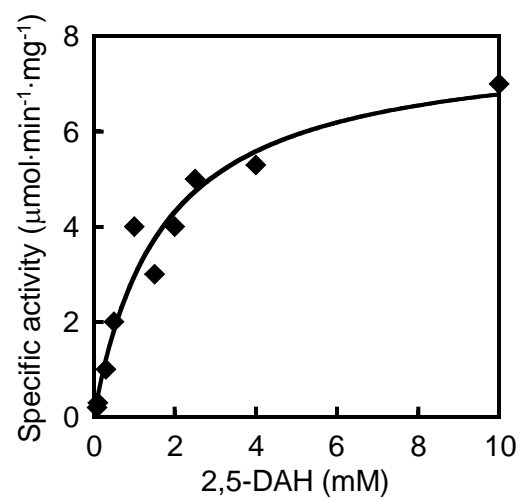


Figure 5

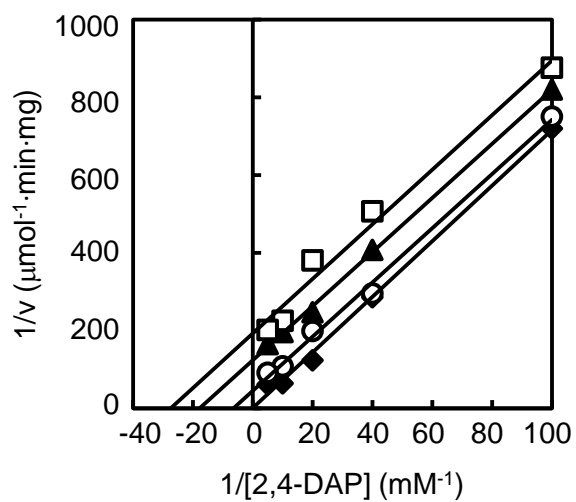


Figure 6

1    Table 1. Effects of various reagents on the activity of 2,4-DAPDH

	Relative activity (%) <sup>a</sup>
None	100 ± 0
EDTA	98 ± 6
MgSO <sub>4</sub>	65 ± 11
CaCl <sub>2</sub>	85 ± 7
FeCl <sub>2</sub>	84 ± 4
MnCl <sub>2</sub>	104 ± 0
CoSO <sub>4</sub>	34 ± 4
NiSO <sub>4</sub>	2 ± 1
CuSO <sub>4</sub>	0 ± 0
ZnSO <sub>4</sub>	2 ± 2
KCl	97 ± 4
KBr	97 ± 5
KNO <sub>3</sub>	93 ± 2
CH <sub>3</sub> COOK	96 ± 4
K <sub>2</sub> SO <sub>4</sub>	96 ± 5

2    <sup>a</sup> The values are shown as the mean ± standard deviation of three independent experiments.

1    Table 2. Kinetic parameters of 2,4-DAPDH

	$K_m$ (mM)	$K_i$ (mM)	$V_{max}$ ( $\mu\text{mol}\cdot\text{min}^{-1}\cdot\text{mg}^{-1}$ )	$k_{cat}$ ( $\text{s}^{-1}$ )	$k_{cat}/K_m$ ( $\text{mM}^{-1}\cdot\text{s}^{-1}$ )
NAD <sup>+</sup>	0.05	-	97	65	1,300
NADP <sup>+</sup>	2	-	86	57	29
2,4-DAP	0.2	0.9	180	65	330
2,5-DAH	2	-	0.9	0.0006	0.0003

2